Isotactic Poly(1-butene)/Hydrogenated Oligo(cyclopentadiene) Blends: Miscibility, Morphology, and Thermal and Mechanical Properties

S. CIMMINO, M. L. DI LORENZO, E. DI PACE, C. SILVESTRE

Istituto di Ricerca e Tecnologia delle Materie Plastiche, IRTEMP CNR, Via Toiano 6, 80072 Arco Felice (NA), Italy

Received 27 February 1997; accepted 27 June 1997

ABSTRACT: The article discusses the influence of the oligomeric resin, hydrogenated oligo(cyclopentadiene) (HOCP), on the morphology and properties of its blends with isotactic poly(1-butene) (PB-1). PB-1 and HOCP are found to be partially miscible in the melt state. Solidified PB-1/HOCP blends contain three phases: (1) a crystalline phase formed by PB-1 crystals; (2) an amorphous PB-1-rich phase; and (3) an amorphous HOCP-rich phase. The optical micrographs of the solidified blends show a morphology constituted by microspherulites and domains of the HOCP-rich phase homogeneously distributed in the intraspherulitic region. DSC and DMTA results show two glass transition temperatures (T_g), different from the T_g values of the plain components. The lower T_g is attributed to the PB-1-rich phase, and the higher T_g, to the HOCP-rich phase. The tensile properties were investigated at 25 and 80°C. At 25°C, the PB-1-rich phase is rubbery and the HOCP-rich phase is glassy, so the addition of HOCP to PB-1 arouses a noteworthy hardening of the samples and this brings an increase of the Young's modulus, E' (although the blend crystallinity lessens), and decreases of stresses at yielding point (σ_y) and at rupture (σ_r). The 90/10 and 80/20 blends show high values of elongation at rupture (ε_r). At 80°C, the blends show decreases of E' and σ_r values with the HOCP content. These decreases are attributed to the rubbery state of the phases and reduction of the blend's crystallinity. At 80°C, all the blends show a high value of ε_r. This phenomenon is attributed to the fine-size domain dispersion of the phases and to sufficient densities of tie molecules and entanglements. Finally, the partial miscibility behavior proposed in this article is compared with the miscibility hypothesis reported elsewhere. © 1998 John Wiley & Sons, Inc. J Appl Polym Sci **67:** 1369–1381, 1998

Key words: poly(1-butene); hydrogenated oligo(cyclopentadiene); resin; blends; miscibility

INTRODUCTION

Isotactic poly(1-butene) (PB-1) is a semicrystalline polyolefin with some interesting properties. Properly molded and processed articles made from poly(1-butene) show excellent resistance to creep and environmental stress cracking.[1] Extruded PB-1 is, in fact, used mainly in the manufacture of pipes and tubes for its impact and corrosion resistance. But other products, such as heavy-duty bags, pressure-sensitive tapes, agricultural films, gaskets, and diaphragms can also be obtained. In certain cases, such as applications at low temperature where high impact resistance is needed, the PB-1 is preferred to iPP and P4MP1 for the production of house furnishings, electrical apparatus, automotive parts, and other articles.[2] PB-1 may crystallize in at least three distinct crystalline modifications.[1] From the melt, PB-1

Correspondence to: S. Cimmino (cimmino@mail.irtemp.na.cnr.it).

Journal of Applied Polymer Science, Vol. 67, 1369–1381 (1998)
 CCC 0021-8995/98/081369-13

crystallizes in the tetragonal crystal modification (form II) and then it transforms into the stable hexagonal crystal modification (form I). Form I generally melts at about 130–138°C, whereas form II melts at lower temperatures, at about 110–115°C. The phase-transformation process from form II into form I starts soon after the crystallization of form II and generally is completed in 1 week at room temperature. The third polymorph (form III) has an orthorhombic unit cell and can be obtained by precipitating the polymer from various solvents.

The hydrogenated oligo(cyclopentadiene) (HOCP) is a commercial amorphous resin, with T_g at about 85°C. It is a mixture of the *cis* and *trans* isomers that after oligomerization have been hydrogenated.

This work is part of a major research concerning the study of the influence of HOCP on the miscibility and properties of semicrystalline polyolefins $(-CH_2-CHR-)_n$ with different side groups R. In previous works, we studied the influence of the resin HOCP on the morphology and thermal and mechanical properties of its blends with isotactic polypropylene[3–6] (iPP) (side group $R=CH_3$), with high-density polyethylene (HDPE)[7,8] (side group R=H), and with poly(4-methylpentene-1) (P4MP1)[9] [side group $R=CH_2CH(CH_3)_2$].

iPP/HOCP[3–6] is a complex polymer system. A phase diagram with both the lower and upper cloud point curves was obtained; depending on temperature, blend composition, and cooling rate from the melt, the system can present one or two amorphous phases in the melt and in the glassy state. iPP can assume the smectic form or can crystallize in the monoclinic form. The thermal, dynamic-mechanical, and tensile properties behaviors were found to depend strongly on the composition and thermal history of the samples according to the phase diagram.

HDPE/HOCP blends[7,8] were found, at all temperatures investigated, to separate in the melt in two phases: the HDPE-rich phase and the HOCP-rich phase. At the crystallization temperatures, the HDPE crystallizes from both phases; the thermal, dynamic-mechanical, and tensile properties behaviors were accounted for according to the partial miscibility found for this system.

P4MP1 and HOCP[9] were found not miscible in the melt state. The optical micrographs of the solidified blends showed a morphology constituted by P4MP1 microspherulites and small HOCP domains homogeneously distributed in the intrasperulitic region. DSC and DMTA results showed that the blends present two glass transition temperatures (T_g) equal to the T_gs of the pure components.

The present article reports the results of an investigation concerning the influence of HOCP on the miscibility, dynamic-mechanical properties, and the tensile stress–strain behavior of its blends with PB-1, a polyolefin with side-chain group $R=CH_2CH_3$. The PB-1/HOCP system has been already studied by Canetti et al.[10] and Bonfatti et al.[11] In particular, Canetti et al.[10] studied the influence of HOCP resin on the kinetics of crystal transformation of PB-1 from form II to form I in isothermally crystallized blends. They found that the kinetics of transformation from form II to I decreased with the presence of HOCP in the blends. This result was accounted for by assuming that the HOCP and PB-1 components are miscible in the melt and that the presence of HOCP in the melt reduces the molecular mobility of PB-1 molecules. The influence of HOCP on the crystallization and thermal behavior of thin films of PB-1/HOCP blends was studied.[11] The blends showed a single T_g, depending on composition, and the addition of HOCP effected the decrease of the overall crystallization rate, the spherulite growth rate, and the equilibrium melting temperature. These results were accounted for by assuming that the two components were miscible in the amorphous state and the miscibility was due to specific interactions between the two components.

The primary objectives of this article are to investigate the miscibility and other properties of the PB-1/HOCP blends by the combination of optical microscopy, differential scanning calorimetry, and dynamic-mechanical, thermal, and the stress–strain tensile analyses. Our interest derives from the consideration that we have already found that HOCP is partially miscible with iPP and HDPE and not miscible with P4MP1 at all compositions investigated. The size of the side-chain group —R of PB-1 is larger than those of iPP and HDPE and smaller than that of P4MP1. A large difference of the volume units of the components corresponds to conspicuous differences in the free volume and the thermal expansion coefficient. As shown by McMaster,[12] small differences of the thermal expansion coefficient lead to complete immiscibility. Moreover, we also consider that there is no possibility of any specific interactions between the repeat units of each component, as is supposed in ref. 11. Therefore, either partial miscibility or complete immiscibility would be expected for the PB-1/HOCP blends studied in this article.

EXPERIMENTAL

Materials

Isotactic poly(1-butene) (PB-1) was produced by Scientific Polymer Products Inc.: $M_w = 1.85 \times 10^5$ (g mol^{-1}), density 0.915 (g cm^{-3}), melt index 20, $T_g = -24 \pm 3$°C (measured by DSC), and $T_m = 125$°C (form I) (measured by DSC). Hydrogenated mixtures of isomers of oligo(cyclopentadiene) (HOCP), Escorez 5120, was produced by Esso Chemical Co. It has an $M_w = 630$, $T_g = 85 \pm 3$°C (measured by DSC), and density = 1.07.

Blend Preparation

The PB-1 and HOCP components were mixed in a Brabender-like apparatus (Rheocord EC of HAAKE Inc.) at 160°C and 32 rpm for 10 min. PB-1/HOCP blends with weight ratios (w/w) of 100/0, 90/10, 80/20, 60/40, and 40/60 were prepared. DSC measurements were performed using these samples.

Preparation of Compression-Molded Sheets

The blends were compression-molded in a heated press at 160°C for 5 min without any applied pressure, to allow complete melting. After this period, a pressure of 100 bar was applied for 5 min, then the platens were quenched with water and the pressure was released. Samples cut from the rectangular sheets ($1 \times 60 \times 120$ mm) were used for the optical microscopy, DMTA, and tensile experiments.

Optical Microscopy

The morphology of the blends was studied by using a Zeiss Axioscop polarizing optical microscope, fitted with a Linkam TH600 hot stage. Thin films were obtained by squeezing a thin slice of compression-molded sheets between two microscope cover glasses. The films so obtained were then heated and cooled under a nitrogen purge at 20°C/min.

Calorimetric Measurements

Thermal properties of the blends were measured with a differential scanning calorimeter Mettler DSC-30. About 10–15 mg of each sample was heated from −80 to 200°C at a scanning rate of 20°C/min. The T_g value was taken as the temperature corresponding to the maximum of the peak obtained by the first-order derivative trace. The observed melting temperature (T_m) was measured at the maximum of the endothermic peak.

Dynamic Mechanical Test

Rectangular specimens ($1 \times 6 \times 30$ mm) were cut from the compression-molded sheets. Dynamic-mechanical tests were performed at 1 Hz and at a heating rate of 4°C/min from −80°C to 100°C under a nitrogen purge with a DMTA-Polymer Laboratories MKIII tester configured for automatic data acquisition. The experiments were performed in a bending mode.

Tensile Tests

Dumbbell-shaped specimens were cut from the sheets and used for the tensile measurements. Stress–strain curves were obtained by an Instron machine (Model 1122) at 25 and 80°C and at crosshead speed, V_t, of 10 mm min^{-1}, gauge length = 22 mm, and nominal strain rate = 0.45 min^{-1}. Modulus, stress, and strain at yield and at rupture were calculated from such curves from an average of 10 specimens.

RESULTS AND DISCUSSION

Morphology and Phase Structure

Optical analyses of the melt of pure PB-1 and blends were carried out from the melting point up to 350°C, where all the samples are still thermally stable under a nitrogen atmosphere for times much longer than those used here for the optical observations. Figure 1(a) shows the melt of PB-1 at 250°C and it is reported as an example of the homogeneity observed in the melt. Figure 1(b) shows the morphology observed when the same melt is cooled to 25°C (cooling rate of 20°C/min). The PB-1 is now crystallized according to a spherulitic morphology. Large and small spherulites are present. The presence of spherulites of different sizes is known to occur when the nucleation processes are time- and temperature-dependent. In fact, during the cooling, at high T, the presence of a few nuclei induce the formation of early spherulites that can grow further, and these are the large spherulites present in the figure. At lower temperature, a large number of nuclei induce the growth of many spherulites that cannot grow to large size.

Optical micrographs of 90/10 blends at differ-

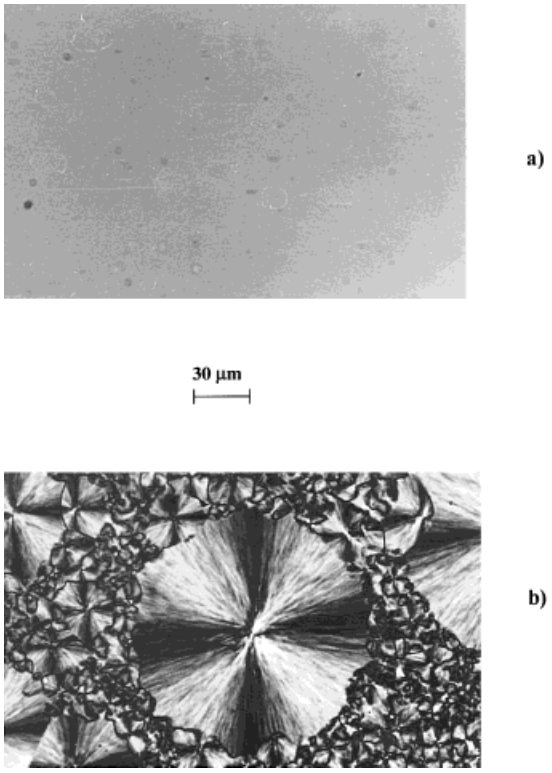

Figure 1 Optical micrographs of PB-1 film: (a) sample at 250°C; (b) sample at 25°C.

ent temperatures are shown in Figure 2. Up to about 250°C, the melt of the 90/10 sample shows the presence of small droplets homogeneously distributed in the matrix [see Fig. 2(a)]. Increasing the temperature above 250°C, the droplets decrease in size, until at about 270°C, the melt becomes and remains homogeneous and transparent up to 350°C [see Fig. 2(b)]. Cooling this sample from 350°C, the droplets appear again at about 270°C, and with continuous cooling, they increase in size and the morphology of the melt becomes the same as that shown in Figure 2(a). When the blend sample is cooled to room temperature, large and small spherulites are also observed [see Fig. 2(c)], but their textures are different from those observed for pure PB-1. They are coarse and much smaller. Furthermore, observations of the same region of this blend sample, carried out during the cooling, changing from cross to parallel polarization conditions and vice versa, indicate that the crystals grow within a liquid–liquid phase-separated melt, as that shown in Figure 2(a), and the droplets are included in the intraspherulitic regions during the crystallization.

Figure 3 shows the optical micrographs of the 80/20 blend in the melt at 150 and 250°C and the morphology of the sample cooled to 25°C. The melt of the 80/20 is characterized by the presence of numerous droplets, as shown in Figure 3(a). By increasing the temperature in the range 200–250°C, some droplets coalesce together and the morphology becomes like that shown in Figure 3(b) and remains the same until 350°C. When the sample is cooled to 25°C, the morphology obtained is that shown in Figure 3(c), where only microspherulites are present. Optical observations carried out during the cooling to 25°C, switching

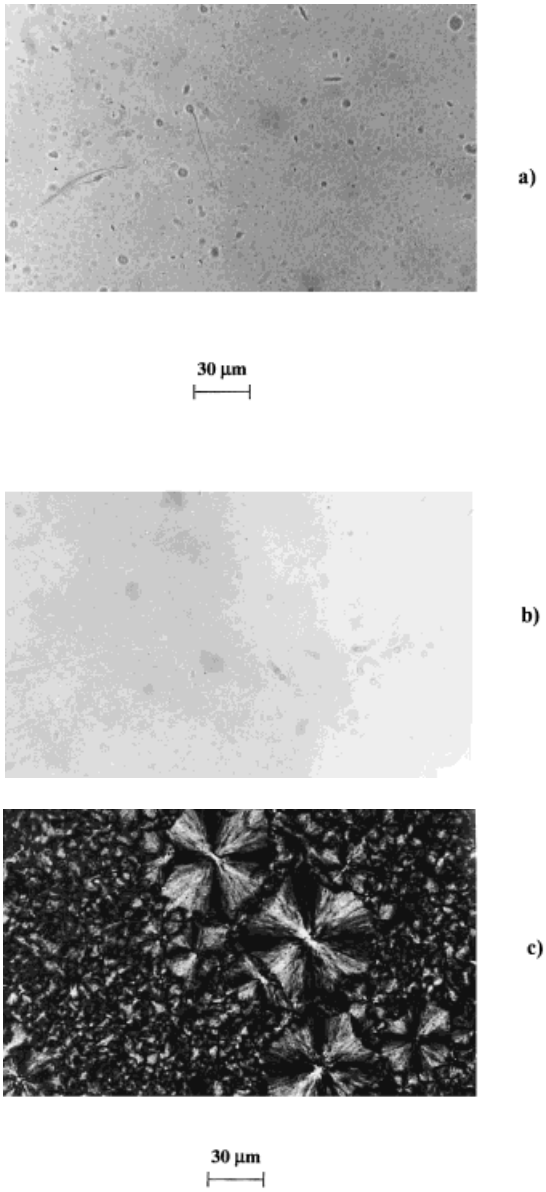

Figure 2 Optical micrographs of 90/10 blend film: (a) sample at 200°C; (b) sample at 300°C; (c) sample at 25°C.

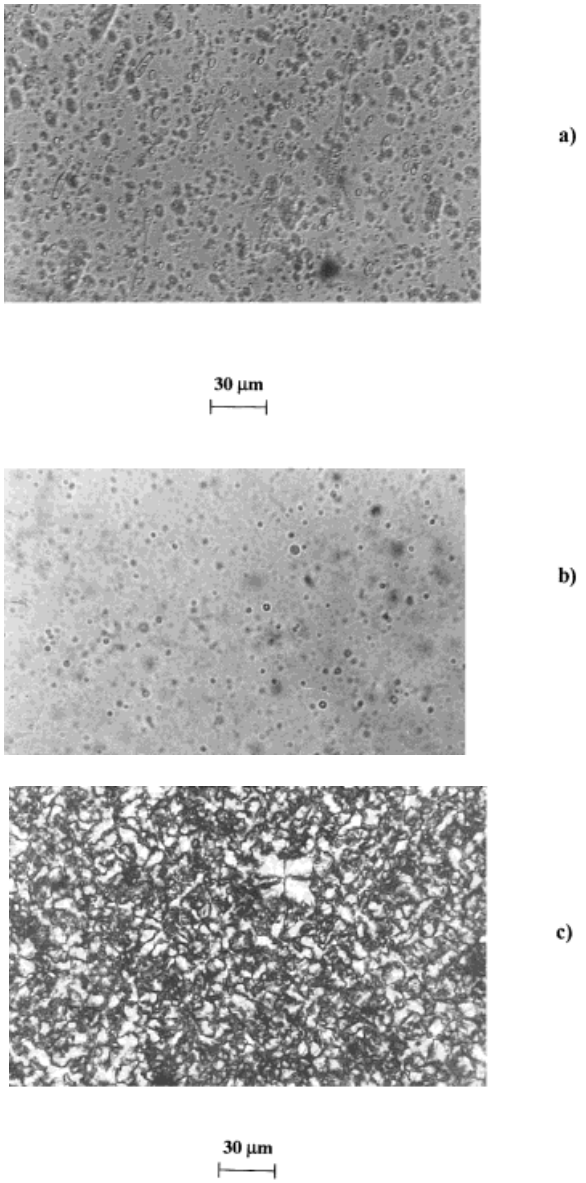

Figure 3 Optical micrographs of 80/20 blend film: (a) sample at 150°C; (b) sample at 250°C; (c) sample at 25°C.

from cross to parallel polarization conditions and vice versa, show that the droplets are included in the intraspherulitic region. Experiments similar to those carried out on the 80/20 blend were performed on 60/40 and 40/60 blends. The optical micrographs of these blends are reported in Figures 4 and 5, respectively.

The optical microscope observations performed on these two last blends indicate the presence in the melt of small and large droplets [see Figs. 4(a,b) and 5(a,b)]. The micrographs of these samples cooled to 25°C indicate a morphology texture constituted by microspherulites and by droplets homogeneously distributed, as shown in Figure 4(c,d) for the 60/40 blend and Figure 5(c,d) for the 40/60 blend.

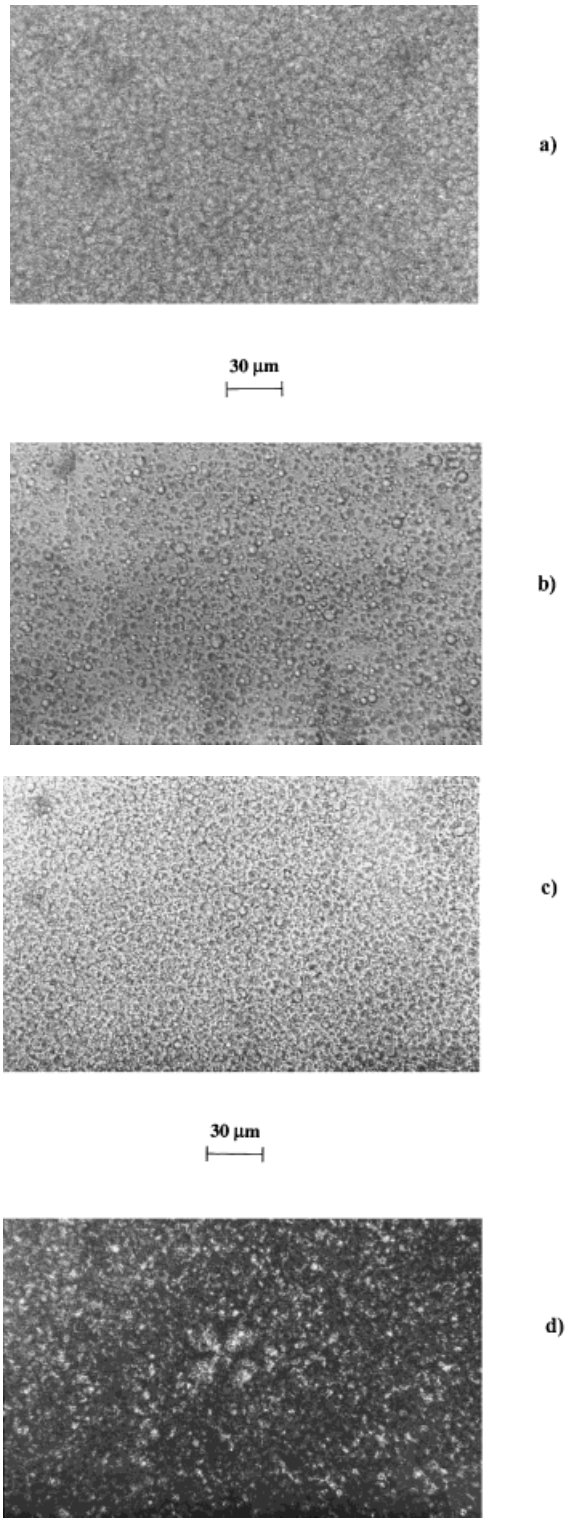

Figure 4 Optical micrographs of 60/40 blend film: (a) sample at 150°C; (b) sample at 250°C; (c) sample at 25°C, parallel polars; (d) sample at 25°C, crossed polars.

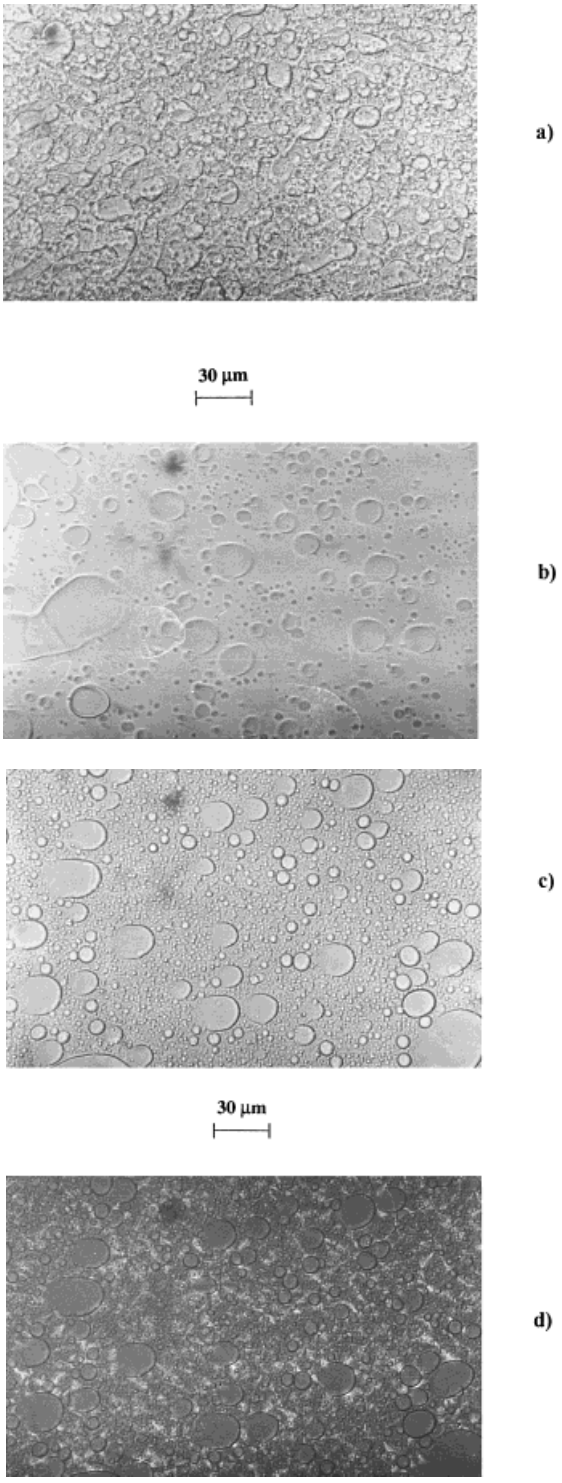

Figure 5 Optical micrographs of 40/60 blend film: (a) sample at 180°C; (b) sample at 250°C; (c) sample at 25°C, parallel polars; (d) sample at 25°C, crossed polars.

Thermal Behavior

The DSC curves of neat PB-1, tested at different times after the processing in the Rheocord, are reported in Figure 6. The curve labeled "a" in Figure 6 was performed soon after the mixing of PB-1 in the Rheocord. An endothermic peak centered at about 115°C is observed and indicates the presence of the only form II in the sample. The crystalline percentage of this sample is found to be about 22% (ΔH_f of form II = 18 cal/g [ref. 13]). Curve "b" was performed 1 day after the mixing, and it shows the presence of both forms II and I. Finally, curve "c" was performed after 1 week and shows the presence of form I only and the percent crystallinity is 43% (ΔH_f of form I = 30 cal/g [Ref. 13]). For the blends, the phase transformation seems to proceed in two steps: In the first step, the transformation rate is high and almost equal to that of plain PB-1, whereas in the second one, the rate is low. Soon after the melt is cooled to room temperature, a partial transformation is observed in times almost equal for all the blends (about 1 week). An example of this situation is shown in Figure 7 (60/40 blend), where the peaks at higher and lower temperature indicate the presence of a large amount of form I and a low percentage of form II, respectively. It is observed that the residual form II transforms to form I at a very slow rate; in fact, a very small peak is still present after 1 month in the DSC curve. Only after 4 months does the phase transformation seem complete and a percent crystallinity of approximately 43% (with reference to PB-1) attained. Moreover, the temperatures of the peaks of the forms II and I decrease as the HOCP content increases. The phase transformation from form II to I was already studied by Canetti et al.[10] in isothermally crystallized blends.

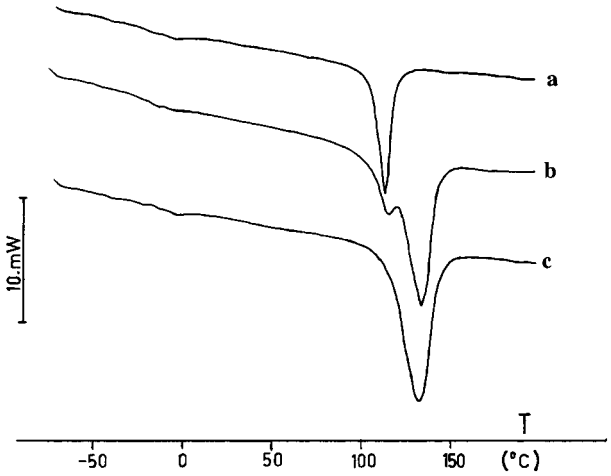

Figure 6 DSC thermograms of PB-1: (a) scan carried on soon after the mixing; (b) after 1 day; (c) after 1 week.

In Table I (second column), the T_gs of the PB-1/HOCP blends as obtained by DSC are reported. The neat PB-1 has the glass transition at about −23°C, whereas for the blends, two T_gs are always found, whose values do not depend on the time elapsed after the mixing, indicating that the phase transformation from form II to form I does not influence the T_gs of the blends. In particular, for the 90/10 blend, the lower T_g is at about −15°C and the upper at about 40°C, whereas the other blends show the lower at about −10°C and the upper at 50°C.

Dynamic-Mechanical Thermal Analysis

The loss tangent (tan δ) and the storage modulus (E') of the PB-1/HOCP blends are reported in Figures 8 and 9, respectively. DMTA experiments for pure HOCP are not possible because compression-molded samples cannot be obtained due to its low molecular weight. The tan δ curve of PB-1 (curve a) shows only one peak, with a maximum at about −5°C, and it represents the T_g of PB-1. The 90/10 blend (curve b) shows only one peak, although smaller than that of PB-1 in magnitude and it is slightly shifted to higher temperature with the maximum at about +5°C. The tan δ curve of the 80/20 blend (curve c) shows the presence of a second, diffuse peak, extending in the temperature range 60−70°C, whereas the first peak still decreases in magnitude and moves a little to higher T. Increasing the HOCP content in the blends (see the curves of the 60/40 and 40/60 blends), the second peak increases remarkably in magnitude, showing now a well-defined maximum, centered at about 70°C, whereas the first peak decreases in magnitude. The analysis of E' values shows a plateau at low temperatures whose temperature range increases with HOCP (see Fig. 9). After the plateau, depending on composition and temperature range, different slopes of the modulus are observed. The storage modulus of the blends at temperatures lower than the T_g of HOCP is higher than that of neat PB-1, E' increasing with HOCP content. The opposite is true at temperatures very close or higher than the T_g of HOCP, as would be expected.

The optical microscope, DSC, and DMTA analyses could be accounted for by assuming that the PB-1 and HOCP components in the blends are not completely miscible in the melt. The melt at mixing temperature separates in two phases: One is the PB-1-rich phase and the other is the HOCP-rich phase. Only for the 90/10 blend, it is found that the two components become miscible at $T > 270$°C, at least for the resolution power of the optical microscope used. At room temperature, the PB-1/HOCP blends contain also a third phase constituted by PB-1 crystals. According to this hypothesis, the droplets observed in the melts of the blends are constituted by the HOCP-rich phase, whose glass transition is revealed by the higher-temperature transition on the DSC thermogram and by the second peak of tan δ. The continuous phase observed in the optical micrographs of the blends is constituted by a homogeneous phase formed by PB-1 and a small amount of HOCP. The T_g of this phase is indicated by the first peak of tan δ and by the first glass transition on the DSC thermogram.

The presence of two T_gs for the blends influences the trends of E' reported in Figure 9. In

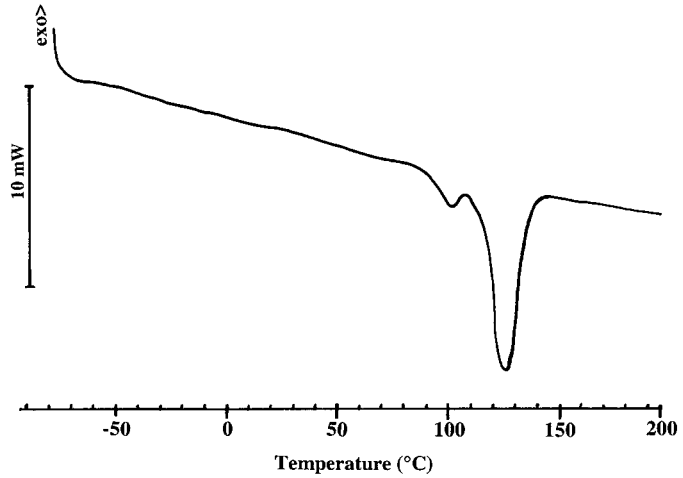

Figure 7 DSC thermogram of 60/40 PB-1/HOCP blends performed after 1 month from the mixing.

Table I Glass Transition Temperature, Melting Point of Form I, and Crystallinity Index of PB-1/HOCP Samples

PB-1/HOCP (w/w)	T_g (°C) by DSC ±3		T_g (°C) by DMTA ±2		T_m (Form I) (±1°C)	X_c (PB-1, Form I) (±3%)
100/0	−23		−5		132	43
90/10	−15	40	5		130	41
80/20	−10	50	10	60–70	130	41
60/40	−10	50	10	70	127	41
40/60	−10	50	10	70	125	
0/100	85		110–120			

fact, at low temperatures, the plateau of the E' curve of each blend increases with the HOCP content. Soon after the plateau (i.e., at $T > T_g$) the storage modulus of the PB-1 sample falls abruptly because the glassy amorphous phase of PB-1 becomes rubbery. After this sudden decrease, the modulus lessens slightly with the temperature due the presence of the PB-1 crystalline phase in the sample. For the blends, the storage modulus does not decrease so abruptly after the T_g, but it diminishes at a higher temperature (this is particularly evident for the 60/40 and 40/60 blends) because the presence of the glassy HOCP-rich phase contributes to keep the modulus high, although the total crystallinity of the sample decreases. At temperature higher than 80°C, the HOCP-rich phase becomes rubbery and so the modulus shows a further decrease and the values are lower for the blends with less crystallinity content.

Tensile Analysis

Physical properties of crystallizable polymer blends depend markedly on the composition, on the supercrystalline morphology, and on level of the phase segregation that result from crystallization and potential phase-separation processes in the amorphous phase. In the case of compatible blends of multicomponent polymer systems presenting amorphous phase separation besides the crystalline phase, the large-strain properties such as the elongation at break or the toughness are particularly related to the homogeneity level of the phases present in the material. The low-strain properties, such as the Young's modulus and

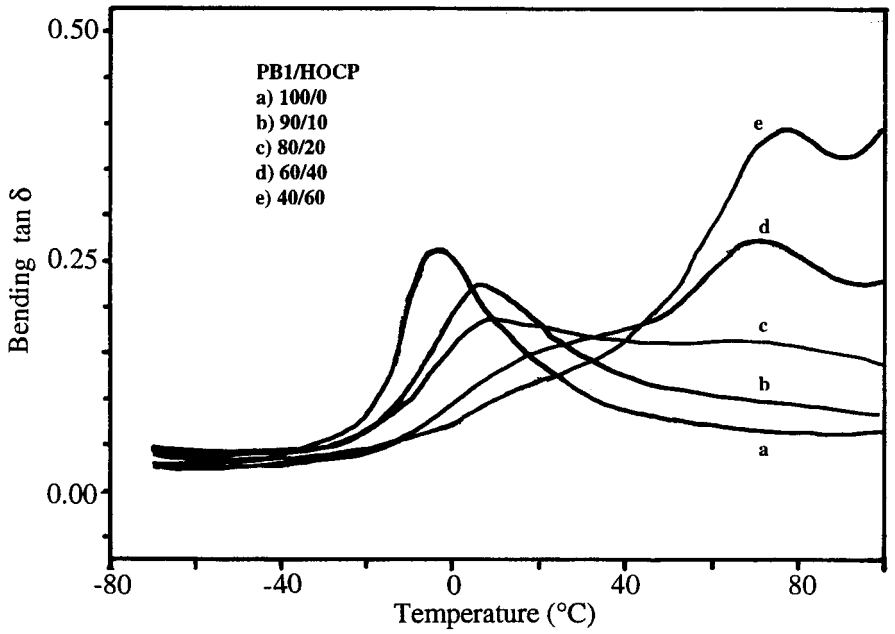

Figure 8 Loss tangent of PB-1/HOCP blends.

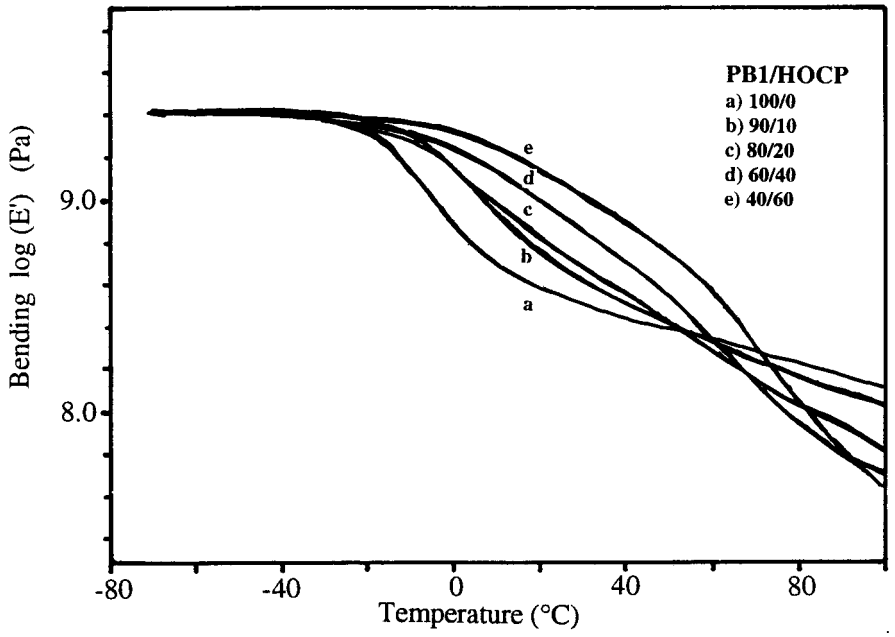

Figure 9 Storage modulus of PB-1/HOCP blends.

yielding parameters, are much less dependent on the homogeneity of the phases. So, in the case of polymer blends, where, besides the crystalline phase, two or more amorphous phases are present, good tensile properties such as tensile strength and yield and ultimate parameters could be expected if domains are small in size and well dispersed in the continuous phase.

On the basis of the optical morphology evidence showing that the two amorphous phases and the crystalline phase have a good level of homogeneity, it is expected that the PB-1/HOCP blends, depending on composition, should have acceptable tensile properties. The tensile analysis was carried out at room temperature (where the PB-1-rich phase is rubbery and the HOCP-rich phase is glassy) and at 80°C (where both phases are rubbery). To have the most possible homogeneity of the crystalline form of PB-1 crystals in the materials, the samples were kept at room temperature, before being subjected to the tensile test, for at least 4 months in order to permit the complete transformation of form II to I.

Nominal stress–strain curves of PB-1 and the PB-1/HOCP blends tested at 25 and 80°C are presented in Figures 10 and 11, respectively. The Young's modulus, yield stress (σ_y) and elongation (ε_y), and tensile (σ_r) and elongation (ε_r) parameters are summarized in Table II (25°C) and Table III (80°C). At 25°C, the PB-1 sample and the blends containing HOCP up to 40% show ductile behavior; the Young's modulus increases with the HOCP percentage, whereas the σ_y and σ_r values decrease. The elongation at yield (ε_y) and at break point (ε_r) of the 90/10 and 80/20 blends are almost similar to those of neat PB-1. The 40/60 blend (curve e) presents a brittle behavior characterized by a low value of ε_r. The tensile behaviors at 25°C can be accounted for by considering that at 25°C the blend sample is constituted by the crystalline PB-1 phase, the rubbery PB-1-rich phase ($T_g \cong -10$°C, by DSC), and the glassy HOCP-rich phase ($T_g \cong 50$°C, by DSC), whose amount increases with HOCP. So, the addition of HOCP to PB-1 causes hardening of the material. This brings an increase of the Young's modulus and decreases σ_y and σ_r for the blends. The similar values of ε_r of the 90/10 and 80/20 blends (values similar to neat PB-1 sample) are probably due to the fine-size domain dispersion of the phases present in the samples (as shown in Figs. 1–5) and to elevated densities of entanglements and tie molecules still present in the sample blends although the 10 and 20% of PB-1 is substituted with HOCP. These factors contribute to the high elongation, almost to that of PB-1. The 40/60 blend contains a large amount of the glassy HOCP-rich phase and that makes it very brittle.

Nominal stress–strain curves of PB-1 and PB-1/HOCP blends tested at 80°C are shown in Figure 11. At this temperature, both amorphous phases are rubbery. It is observed that E' and σ_r values (see also Table III) decrease as the HOCP content in the blends increases. Both amorphous

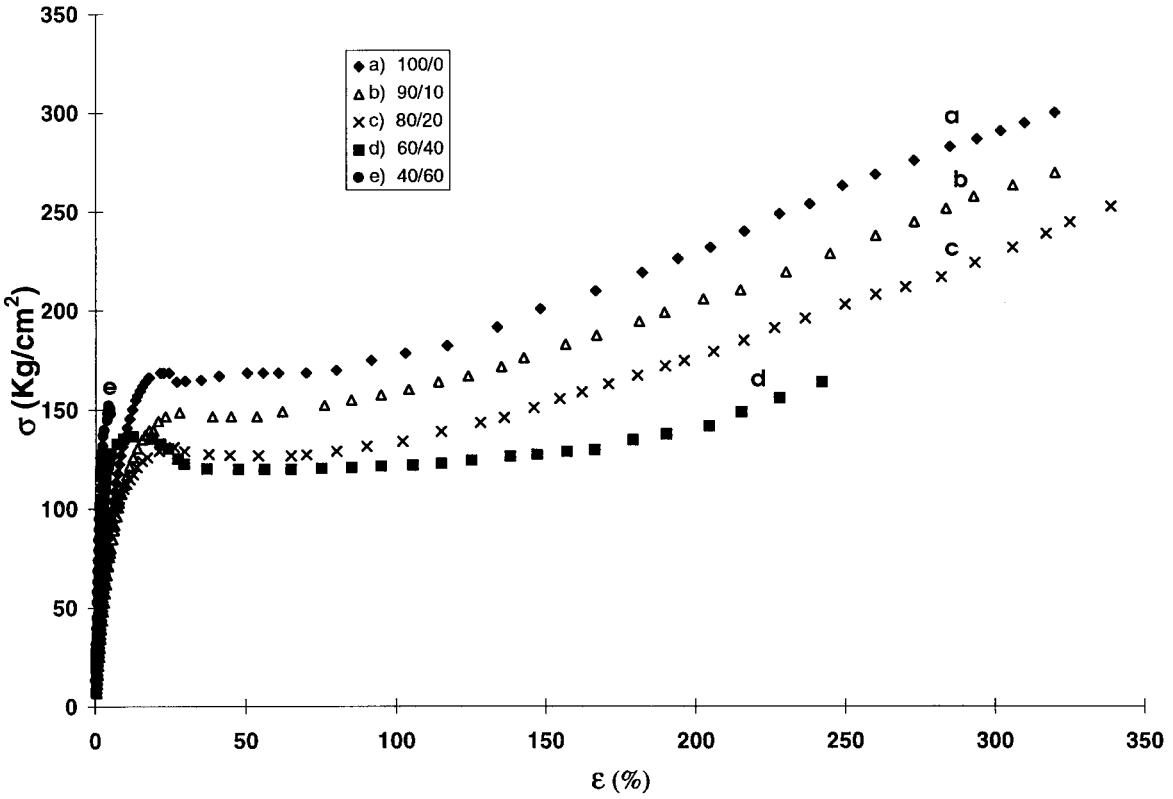

Figure 10 Stress–strain curves PB-1/HOCP blends at 25°C.

phases are now rubbery and the addition of HOCP reduces the overall crystallinity of the blends, which lowers the values of E' and σ_r. These factors affect also the yield phenomenon, presented only by PB-1 and the 90/10 blends. These results seem to indicate that, besides the fine-size domain dispersion of the phases present in the materials with high HOCP content, there should be a sufficient density of tie molecules that interconnect the crystalline domains of PB-1 and also a sufficient density of entanglements that interlace the amorphous phases, to permit high elongation before the rupture.

CONCLUSIONS

The observations of the optical microscopy and the results of the DSC and DMTA analyses have shown that the PB-1 and HOCP components do not form a miscible system in the melt state but two conjugated phases: the PB-1-rich phase and the HOCP-rich phase. Moreover, after crystallization, the solidified samples contain a third phase composed of PB-1 in tetragonal modification that transforms to the more stable hexagonal modification with time. For all the blend compositions studied, it is found that in the melt and in the solid state the domains of the HOCP-rich phase are small and homogeneously distributed in the matrix. The DSC and DMTA results indicate the presence of two T_gs, whose values are different from those of the two components, and they are attributed to the two amorphous conjugated phases. The tensile properties were investigated at 25 and 80°C. At 25°C, the PB-1-rich phase is rubbery and the HOCP-rich phase glassy, whereas at 80°C, both phases are rubbery. The different behaviors of the tensile properties have been attributed to the composition, the physical state of the amorphous phases, and to the amount of the crystalline phase that decreases with increasing the HOCP in the blends.

FURTHER COMMENTS

Our results have been interpreted with the assumption that PB-1 and HOCP components are not completely miscible in the melt, but they form two conjugated amorphous phases, whereas in ref. 11 the two components are reported miscible

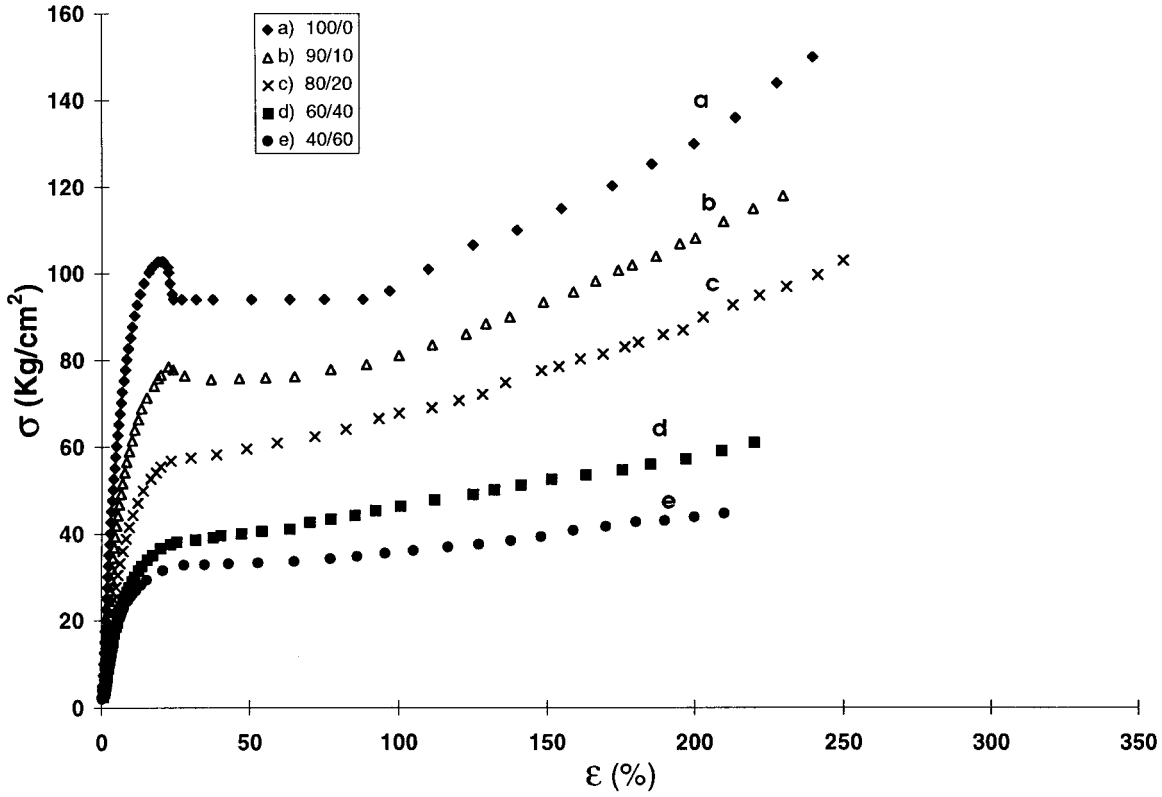

Figure 11 Stress–strain curves PB-1/HOCP blends at 80°C.

in the melt. The main experimental results reported in ref. 11 for the assumption of miscibility are the findings of the melting point depression and one glass transition of the blends by using DSC. The findings that a polymer blend presents an equilibrium melting point depression obtained by Hoffman–Weeks[14] and that the use of the Nishi and Wang equation[15] or others as that proposed by Kwei and Frisch[16] (all expressions derived from the Flory treatment[17]) gives a negative value of the polymer–polymer interaction parameter, χ_{12}, does not mean that the blend is miscible. We found that phase-separated blends can also present an equilibrium melting point depression due to the morphological changes of the crystalline phase and not due to a diluent factor.[18] Of course, in this case, the application of the Nishi and Wang equation gives a negative χ_{12} parameter that is mathematically correct, but erroneous in the meaning. Other authors such as Kalfoglu[19] and Ramsay et al.[20] reported the same considerations.

To elucidate this point, we must consider that the experimental melting point depression in the blends is a result of thermodynamic and kinetic factors. In any crystallizable polymer blend, the thermodynamic factor derives from the thermodynamic rules of mixing of a diluent added to a saturated solution and will be zero for an incompatible blend. The kinetic effect arises because the crys-

Table II Tensile Parameters of PB-1/HOCP Blends at 25°C

PB-1/HOCP (w/w)	E (kg/cm^2)	σ_y (kg/cm^2)	ε_y (%)	σ_r (kg/cm^2)	ε_r (%)
100/0	2130 ± 70	167 ± 4	29 ± 1	302 ± 25	320 ± 20
90/10	2330 ± 30	150 ± 1	30 ± 1	270 ± 20	320 ± 20
80/20	3000 ± 200	131 ± 5	26 ± 1	253 ± 8	335 ± 20
60/40	5000 ± 300	135 ± 4	13 ± 1	160 ± 5	242 ± 5
40/60	6800 ± 300	—	—	148 ± 9	5 ± 1

Table III Tensile Parameters of PB-1/HOCP Blends at 80°C

PB-1/HOCP (w/w)	E (kg/cm^2)	σ_y (kg/cm^2)	ε_y (%)	σ_r (kg/cm^2)	ε_r (%)
100/0	1500 ± 25	102 ± 1	20 ± 2	150 ± 10	240 ± 10
90/10	1020 ± 20	78 ± 2	22 ± 1	118 ± 7	230 ± 10
80/20	660 ± 80	—	—	103 ± 2	250 ± 5
60/40	430 ± 30	—	—	61 ± 4	220 ± 8
40/60	530 ± 2	—	—	44 ± 5	210 ± 13

tals are formed at temperatures below the equilibrium melting point of the polymer mixture (T_m). This latter obviously depends upon the composition of the blends and procedures exist for separating its contribution. One of these involves using the Hoffman–Weeks procedure[14] that has been largely utilized for estimating the equilibrium melting points for many polymer systems as done in ref. 11. The limit of this method is that the experimental melting point depends not only on the crystallization temperature but also on crystallization time (which is never considered in the articles) and, finally, on the blend composition.[21,22] These factors are generally not eliminated by the use of the Hoffman–Weeks method due to its limits.[21–24] In fact, difficulties in fitting the Nishi and Wang equation to equilibrium melting points are generally reported[21,23,25]; the plot of the equation should give a straight line passing through the zero of the axes (the slope gives a χ_{12} value), but the intercept gives always a positive value, as also in ref. 11.

Another (better) procedure to calculate the equilibrium melting point involves measurement of the lamella thickness, l, by small-angle X-ray scattering, then plotting the melting point against $1/l$ and extrapolating to zero.[21] But this method also has some limits that we do not consider here. Finally, whatever is the procedure used, it must consider the limits of the Flory–Huggins theory: (1) χ_{12} is considered independent of composition; (2) the theory is unable to describe the lower critical solution temperature; and (3) the theory does not consider the volume change on mixing, neglecting the free-volume effect. So, the use of the melting point depression procedure to evaluate if a polymer system is miscible or not must be supported by other experimental evidence.

About the single glass transition reported in ref. 11, we note that the 90/10 blend has a $T_g = -20$°C, the T_g of the 80/20 blend is −19°C, and that of the 70/30 is −18°C, i.e., a difference of only 2° between the 90/10 and the 70/30 blends. Considering that the measurement of the glass transition value by DSC has generally an uncertainty of at least 2°, these blends show the same value of T_g. As also shown in ref. 11, the T_gs of these blends are much lower than the values predicted by the Fox equation and this cannot be attributed to any specific interactions, as is supposed in ref. 11, since they are not possible between the components. The T_gs found in ref. 11 are relative to the PB-1-rich phase and the authors cannot observe the second glass transition of the HOCP-rich phase, because it is masked by the crystallization peak that their DSC thermograms (not shown) must present. In fact, the blend samples used in ref. 11 are completely amorphous since they were first melted and then immersed in liquid nitrogen before the T_g experiments. We performed the DSC experiments of the blends following the procedure used in ref. 11 and the thermograms obtained showed the presence of an exothermic peak right in the temperature range where the T_gs relative to the HOCP-rich phase are located.

One of the authors (M.L.D.L.) thanks the CAMPEC–Napoli Consortium for supporting her research at IRTEMP CNR.

REFERENCES

1. I. D. Rubin, in *Poly(1-Butene),* H. Morawtz, Ed., Gordon and Breach, London, 1968, Preface, p. vii.
2. P. Parrini and G. Crespi, in *Encyclopedia of Polymer and Science and Technology,* H. F. Mark, N. G. Gaylord, and N. M. Bikales, Eds., Wiley, New York, 1970, Vol. 13, p. 117.
3. E. Martuscelli, C. Silvestre, M. Canetti, C. de Lalla, A. Bonfatti, and A. Seves, *Makromol. Chem.,* **190,** 2615 (1989).
4. S. Cimmino, P. Guarrata, E. Martuscelli, and C. Silvestre, *Polymer,* **32,** 3299 (1991).
5. S. Cimmino, E. Di Pace, F. E. Karasz, E. Martuscelli, and C. Silvestre, *Polymer,* **34,** 972 (1993).
6. S. Cimmino, E. Martuscelli, and C. Silvestre, *Makromol. Chem. Macromol. Symp.,* **78,** 115 (1994).

7. S. Cimmino, E. Di Pace, E. Martuscelli, L. C. Mendes, and C. Silvestre, *J. Polym. Sci. Part B Polym. Phys.,* **32,** 2025 (1994).
8. S. Cimmino, E. Di Pace, E. Martuscelli, C. Silvestre, L. C. Mendes, and G. Bonfanti, *J. Polym. Sci. Part B Polym. Phys.,* **33,** 1723 (1995).
9. S. Cimmino, M. Monaco, and C. Silvestre, *J. Polym. Sci. Part B Polym. Phys.,* **35,** 1269 (1997).
10. M. Canetti, M. Romanò, P. Sadocco, and A. Seves, *Makromol. Chem.,* **191,** 1589 (1990).
11. A. M. Bonfatti, M. Canetti, M. Sadocco, A. Seves, and E. Martuscelli, *Polymer,* **34,** 990 (1993).
12. L. P. McMaster, *Macromolecules,* **6,** 760 (1973).
13. B. Wunderlich, *Macrolecular Physics,* Academic Press, New York, 1973, Vol. 1, p. 388.
14. J. D. Hoffman and J. J. Weeks, *J. Res. Natl. Bur. Stand. U.S.,* **60,** 13 (1962).
15. T. Nishi and T. T. Wang, *Macromolecules,* **8,** 909 (1975).
16. T. K. Kwei and H. L. Frisch, *Macromolecules,* **11,** 1267 (1978).
17. P. J. Flory, *Principles of Polymer Chemistry,* Cornell University Press, Ithaca, NY, 1953.
18 S. Cimmino, P. Iodice, and C. Silvestre, *Thermochim. Acta,* to appear.
19. N. K. Kalfoglu, *J. Polym. Sci. Part B Polym Phys.,* **20,** 1259 (1982).
20. H. Verhoogt, B. A. Ramsay, and B. D. Favis, *Polymer,* **35,** 5155 (1994).
21. A. Cecere, S. Cimmino, E. Di Pace, E. Martuscelli, and C. Silvestre, in *Second Mediterranean School on Science and Technology of Advanced Polymer Based Material: Lectures,* S. Cimmino, M. Malinconico, E. Martuscelli, and G. Ragosta, Eds., 1991, p. 562.
22. P. Maiti and A. K. Nandi, *Macromolecules,* **28,** 8511 (1995).
23. P. P. Gan and D. R. Paul, *J. Polym. Sci. Part B Polym Phys.,* **33,** 1693 (1995).
24. H. Chen and R. S. Porter, *J. Polym. Sci. Part B Polym Phys.,* **31,** 1845 (1993).
25. S. Cimmino, E. Martuscelli, C. Silvestre, M. Canetti, C. De Lalla, and A. Seves, *J. Polym. Sci. Part B Polym Phys.,* **27,** 1794 (1989).